Suppression of nonradiative recombination in ionic insulators by defects: Role of fast electron trapping in Tl-doped CsI

Junhyeok Bang,[1] Z. Wang,[2] F. Gao,[2] S. Meng,[3] and S. B. Zhang[1]

[1]*Department of Physics, Applied Physics, and Astronomy, Rensselaer Polytechnic Institute, Troy, New York 12180, USA*

[2]*Pacific Northwest National Laboratory, MS K8-93, P.O. Box 999, Richland, Washington 99352, USA*

[3]*Beijing National Laboratory for Condensed-Matter Physics and Institute of Physics, Chinese Academy of Sciences, Beijing 100190, China*

(Received 4 September 2012; revised manuscript received 9 April 2013; published 23 May 2013)

In semiconductors, defects often assist nonradiative relaxation. However, Tl doping can significantly suppress the nonradiative relaxation in alkali halides to increase scintillation efficiency. Without the Tl, it is known that the creation of Frenkel pairs at self-trapped excitons, assisted by excited electron and hole relaxations, is the reason for the nonradiative relaxation. Here we show by first-principles calculation that Tl doping introduces Tl p states inside the band gap to trap the excited electrons. The trapping is highly effective to within several picoseconds, as revealed by time-dependent density functional theory calculations. It alters the nonradiative relaxation process to result in a noticeable increase in the relaxation barrier from 0.3 to 0.63 eV, which reduces the nonradiative relaxation by roughly a factor of 10^5 at room temperature.

DOI: 10.1103/PhysRevB.87.205206 PACS number(s): 71.55.−i, 71.38.Ht, 72.20.Jv, 78.55.Fv

I. INTRODUCTION

Nonradiative recombination (NRR) of excited carriers is one of the most fundamental phenomena in semiconductors and insulators. NRR can quench luminescence and limit photovoltaic device efficiency. Therefore, understanding NRR also has practical importance.[1–3] However, NRR is often complex involving excited carriers. This leads to difficulties in theoretical analysis and identification of its microscopic origin. As such, key knowledge on NRR is often lacking.

In semiconductors, defects are viewed as the cause for NRR.[4,5] However, in alkali halides counterexamples exist. For example, in scintillation material CsI, which is widely used as a high-energy particle detector,[6,7] a minute amount of Tl doping can significantly suppress NRR and increase light emission efficiency.[8,9] This hints that certain types of defects may improve the efficiency of an optoelectric device. Although there have been considerable efforts to understand the role of Tl,[10–16] the underlying mechanism for the NRR suppression is still unclear. Physical processes in which a dopant reduces rather than increases the NRR is critically important to material research, as it offers clues not only for improved scintillation but also for better LED, laser, photovoltaic, and spintronic devices.

In this work, we present a state-of-the-art treatment of the problem, which includes both hybrid functional calculations for the self-trapped hole (STH) and the self-trapped exciton (STE) and, separately, time-dependent density functional theory (TDDFT) calculations for explicit electron relaxation dynamics. Our study reveals two effects of the Tl: First, there exists a large binding between substitutional Tl and STE of 0.88 eV, therefore an STE is bound to Tl until it undergoes a radiative relaxation or NRR. Second, Tl increases the NRR barrier of the trapped STE significantly to prevent the NRR from happening. It is believed that NRR is caused by the creation and migration of Frenkel pairs. Without the Tl, excited electrons at the conduction band minimum (CBM) and holes at the valence band maximum (VBM) assist the creation of the Frenkel pairs through a strong electron-phonon coupling. With the Tl, however, the excited electron is transferred to the Tl p states within several picoseconds. As a result, the carrier-assisted Frenkel-pair formation paths are blocked, leading to significantly enhanced scintillation efficiency.

II. METHODS

Our structural optimization is based on the spin-polarized density functional theory (DFT) with the hybrid PBE0 functional,[17] as implemented in the VASP code.[18] Projected augmented wave potentials[19] are used for ionic pseudopotentials. Wave functions are expended in a plane-wave basis with an energy cutoff of 290 eV. We use a $5 \times 3 \times 3$ supercell that contains 90 atoms with the [100] direction as the long axis to facilitate the study of interstitial diffusion. Γ point is used for the Brillouin zone integration. Tests with different cell size and k-point sampling suggest that the total energy is converged to within 0.01 eV. The ionic coordinates are fully relaxed until the residual forces are <0.03 eV/Å. To mimic electronic excitation, for pure CsI, we perform constrained DFT calculations in which we remove one electron from the VBM and place it at the CBM. For Tl-doped CsI, we place the excited electron at the Tl level. This is a valid approach because our calculation shows that the electron at the CBM instantaneously transfers to the Tl level. To calculate the energy barrier with nudged elastic band along with hybrid functional is currently difficult. Instead, we generated nine atomic configurations between the initial and final states and then relaxed all the atoms in each configuration except for the two diffusing iodine atoms.

A key to the determination of enhanced scintillation is the time required for electron trapping. The recent development of *ab initio* molecular dynamics (MD) coupled with TDDFT[20] makes this possible. Here, we use the TDDFT formalism implemented in the SIESTA code,[21,22] with norm-conserving Troullier-Martins pseudopotentials,[23] the Perdew-Burke-Ernzerhof (PBE) exchange-correlation functional,[24] and a double-ζ polarized local basis set. The real-space grid is equivalent to a plane-wave cutoff energy of 200 Ry. The time step is 24 attoseconds. We use the Ehrenfest approximation

for ion motion. The supercell for defect contains 54 atoms. To prepare for TDDFT input, we perform electron-ground-state MD simulation at room temperature (RT = 300 K) and then constrained DFT with one electron in the CBM.

III. RESULTS: NONRADIATIVE RECOMBINATION PATHS IN UNDOPED CsI

Scintillation is a fundamental physical phenomenon for energetic particle interaction with solids. When a high-energy particle enters a scintillator material, the energy of the particle is transferred to the surroundings by generating electron and hole pairs. In most alkali halide scintillators, the hole can be localized by lattice distortion, leading to the formation of STH. In CsI, the distortion is the bonding between two adjacent iodine atoms [see Fig. 1(a)], to lower the system energy by 0.31 eV relative to undistorted CsI with delocalized hole. The charge contour plot in Fig. 1(a) reveals that the STH state inside the band gap [see Fig. 2(a)] is an antibonding state. An excited electron in the conduction band can bind to the STH to form an STE. The trapped electron is, on the other hand, delocalized over the supercell. Accordingly, the energy lowering of 0.32 eV due to the STE formation is only 0.01 eV larger than that of the STH [see Table I and Fig. 3(a)]. Not only does the STE itself emit light by radiative recombination, but the diffusion of the STH and STE can also lead to the transfer of their energy to other luminescence centers.[25–29]

The STE can also undergo NRR through Frenkel-pair defect formation and diffusion.[30–32] Figures 1(b)–1(d) show the evolution of the atomic structure during the NRR. First, two adjacent I atoms move along the [100] direction in such a way that the two share one anion lattice site, forming a dumbbell (DB) structure (I_i^{DB}). This leaves behind an I vacancy (V_I). We denote this vacancy-interstitial pair as $(V_I\text{-}I_i^{DB})^{first}$. As the I_i diffuses further away along the [100] direction, it can form additional metastable Frenkel pairs such as the one in Fig. 1(c): $(V_I\text{-}I_i^{TR})^{first}$ with one triple-I-atom chain (TR), as well as the one in Fig. 1(d): $(V_I\text{-}I_i^{DB})^{second}$ with an I DB structure. As the process goes on, the I_i eventually encounters a V_I and recombines, leaving their energy to the lattice as heat.

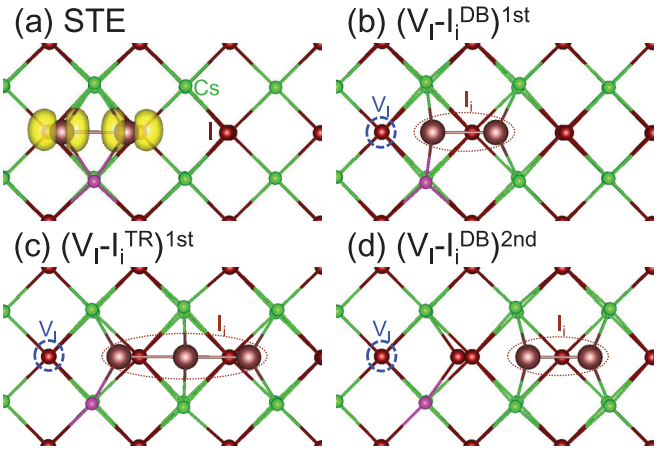

FIG. 1. (Color online) Atomic structures during the I_i diffusion: (a) STE, (b) $(V_I\text{-}I_i^{DB})^{first}$, (c) $(V_I\text{-}I_i^{TR})^{first}$, and (d) $(V_I\text{-}I_i^{DB})^{second}$, where first and second denote the I_i position relative to the V_I. Blue dashed circles denote the V_I's; brown dotted ellipses denote the I_i's. For Tl-doped CsI, the Tl atom replaces the pink Cs atom. In (a), the real-space charge of the STH state [see Fig. 2(a)] is shown by the yellow contours. DB and TR are defined in the text.

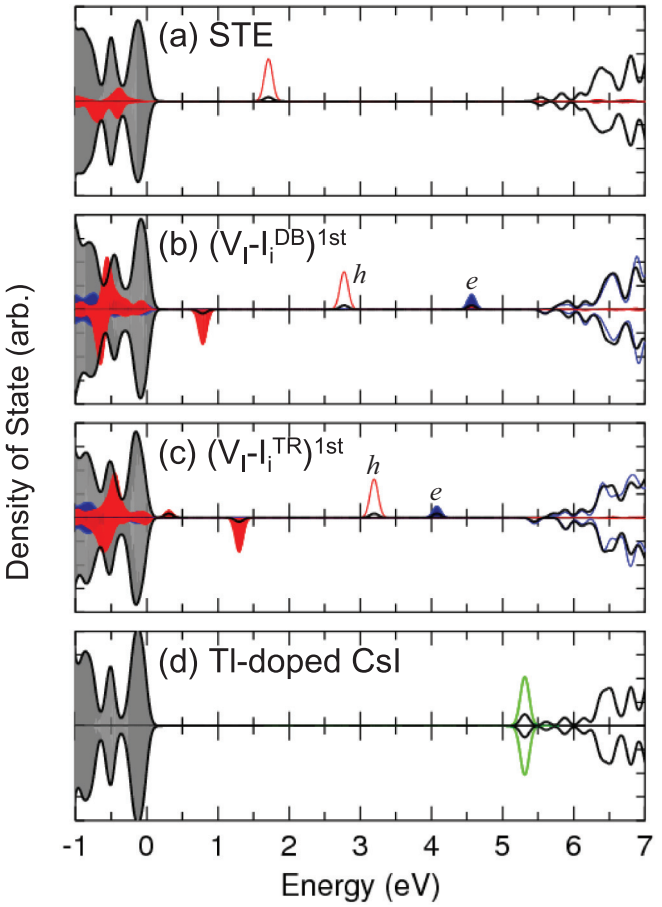

FIG. 2. (Color online) Density of states (DOS) of (a) STE, (b) $(V_I\text{-}I_i^{DB})^{first}$, (c) $(V_I\text{-}I_i^{TR})^{first}$, and (d) Tl-doped CsI. The occupied states are shaded. Red, blue, and green lines denote the projected DOS onto the p states of the I interstitial, the s states of the Cs nearest neighbors to V_I, and the p states of the Tl. All the projected DOS are scaled by a factor of 20 with respect to the total DOS.

Figure 3(a) shows the energy landscape along the NRR path in Fig. 1: From STE to $(V_I\text{-}I_i^{DB})^{first}$, the energy is increased to 0.19 eV; from $(V_I\text{-}I_i^{DB})^{first}$ to $(V_I\text{-}I_i^{TR})^{first}$, the energy is further increased to 0.29 eV. After that, the total energy is nearly flat. The total diffusion barrier for this NRR path [from 1(a) to 1(d) in Fig. 3(a)] is $E_b = 0.30$ eV. The fact that E_b is slightly smaller than the delocalization barrier, 0.37 eV, of the STE [from 1(a) to No STE in Fig. 3(a)] suggests that it prefers NRR over delocalization. By using the rate equation $r = f\ \exp(-E_b/kT)$ and the optical vibration frequency $f = 2 \times 10^{12}\ s^{-1}$ for CsI,[33] we estimate the NRR relaxation time at RT to be 50 ns. This value is on the same order of magnitude with the radiation decay time in CsI.[8,34]

IV. RESULTS: THE EFFECTS OF Tl DOPING

Because of the large binding of 0.88 eV between Tl and STE, Tl doping can significantly affect the formation of STE. A previous study[26] suggested that STE is mobile at RT with a

TABLE I. Energy change at different atomic configurations along the NRR path. Results for CsI with one hole are calculated at the same atomic structures of CsI with one e–h pair to show the effects of the excited electron. The energy is given in unit of eV.

	No self-trapping	Self-trapping	$(V_{\rm I}\text{-}{\rm I}_i^{\rm DB})^{\rm first}$	$(V_{\rm I}\text{-}{\rm I}_i^{\rm TR})^{\rm first}$	$(V_{\rm I}\text{-}{\rm I}_i^{\rm DB})^{\rm second}$
One e–h pair	0.32	STE: 0.0	0.19	0.29	0.29
One hole	0.31	STH: 0.0	0.68	1.15	1.27

barrier as little as 0.15 eV. Thus, STE can be easily trapped at Tl sites, in agreement with experiment.[13,16] Figure 3(b) further shows that Tl doping reduces the STE formation barrier [from No STE to 1(a) in Fig. 3(b)] to <0.01 eV. Hence, most STE exist as Tl-STE pairs.

Tl doping slows down the NRR by increasing the formation energy of Frenkel pairs. We can understand this by examining the evolution of the density of states in Fig. 2 in accordance with that of atomic structures in Fig. 1. Here, we focus on the hole (h) and electron (e) levels marked in Fig. 2, which belong to I_i and V_I, respectively. Going from Fig. 2(a) to Fig. 2(c), the hole level increases; the electron level decreases to enter the band gap. The reason for the change can be attributed to wave-function overlap between e and h, giving rise to level repulsion. As the I_i diffuses away from the V_I, however, the repulsion vanishes. Note that the higher the hole level, the more stable the hole. Thus, throughout the diffusion process in Fig. 1 both the excited electron and hole lower their energies, driving the diffusion forward.

If we remove the excited electron from the system, however, the energy of the Frenkel pairs increases significantly (see Table I). This is precisely what Tl does to slow down and deter NRR. Figure 2(d) shows that the unoccupied p levels of the Tl are below CBM, so the electron in the CBM can be transferred to Tl. Whether such a process is important or not, however, depends on the time required for the transfer. If the time is longer than 50 ns, which is the NRR relaxation time in CsI, then excited carriers will decay nonradiatively. To estimate the electron transfer rate, we performed TDDFT calculations within the PBE functional. Strictly speaking, one may not use PBE here because semilocal functional may not describe charge transfer correctly. Currently, it is still not possible to carry out TDDFT-MD beyond the PBE, such as using a nonlocal hybrid functional. This issue should be considered in future studies.

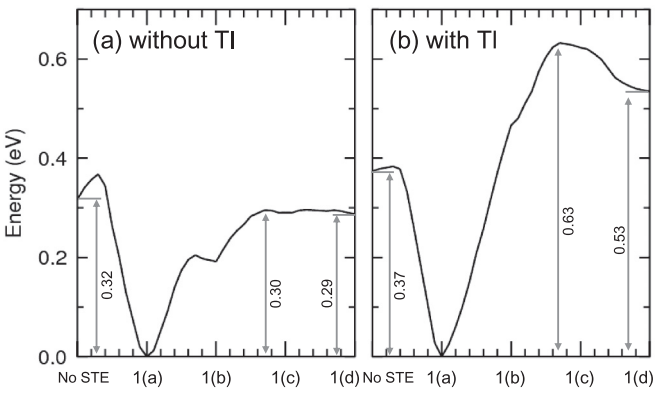

FIG. 3. Total energy landscape along the NRR path for (a) undoped CsI and (b) Tl-doped CsI. The labels in the horizontal axes indicate atomic structures for STE diffusion given in Fig. 1.

Figure 4(a) shows the time evolution of the energy levels for the excited electron in the CBM and the three empty Tl p states.[35] The electron level decreases rapidly towards the Tl p levels, which indicates that electron transfer from the CBM to the Tl p levels has taken place. Accompanied with this electron transfer, ion kinetic energy increases [see Fig. 4(b)]. This is a strong indication that the transfer is mediated by electron-phonon coupling. As a measure of the transfer, Fig. 4(c) shows the change of the amount of electrons in the Tl p levels, defined as $\Delta\rho_{\rm Tl}(t) = \sum_{i=1}^{3}[\rho_{{\rm Tl},i}^{(e)}(t) - \rho_{{\rm Tl},i}^{(g)}]$ where $\rho_{{\rm Tl},i}^{(e)}$ and $\rho_{{\rm Tl},i}^{(g)}$ are the amount of electrons in the Tl p_i states, $|{\rm Tl}, p_i\rangle$, for the excited and ground states, respectively. $\Delta\rho_{\rm Tl}(t=0)$ should be zero if the supercell size is sufficiently large; due to the relatively small cell size and the fact that $|{\rm CBM}\rangle$ and $|{\rm Tl}, p_i\rangle$ are coupled states, however, $\Delta\rho_{\rm Tl}(t=0) = 0.3$ electrons in our simulation. Despite this, the qualitative result, e.g., $\Delta\rho_{\rm Tl}(t)$ increases with time, is not affected. In only 150 fs, $\Delta\rho_{\rm Tl}$ is increased to 0.43 electrons.

Upon excitation, the excited electron stays in the CBM for ~20 fs before significant transfer is noticed in Fig 4(c). This initial waiting is also observed in other materials such as TiO_2.[36] Beyond the initial waiting time t_i, the time evolution of the electron transfer can be modeled by[36] $\Delta\rho_{\rm Tl}(t) = A(1 - \exp[-(t/\tau)])$, where τ is the decay time. As mentioned earlier,

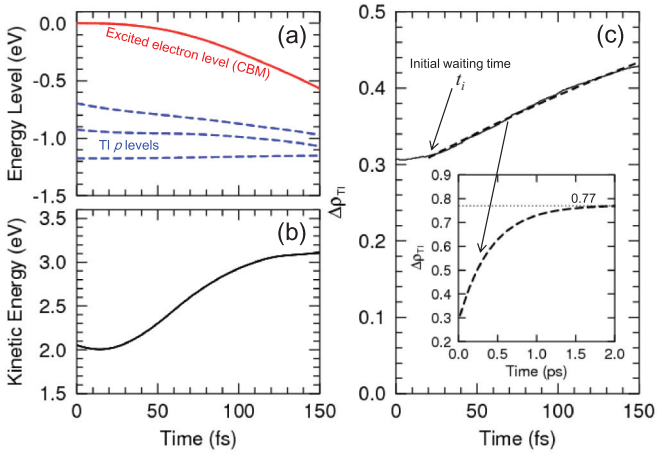

FIG. 4. (Color online) Time evolutions of (a) energy levels, (b) ion kinetic energy, and (c) electron transfer to Tl p levels, $\Delta\rho_{\rm Tl}$. In (a), red and blue lines are the excited electron level and the empty Tl p levels, respectively. In (c), the solid line is the TDDFT result, whereas the dashed line is a fitted result using Eq. (1). t_i is the initial waiting time. The dashed line in the inset in (b) is the same fitting but plotted at a longer time scale. It converges to 0.77 electrons within 2 ps.

$\Delta\rho_{\mathrm{Tl}}(t=0)$ is not zero due to finite cell size; here we modify the above equation to

$$\Delta\rho_{\mathrm{Tl}}(t) = A\left(1-\exp\left[-\frac{t}{\tau}\right]\right)+0.3. \quad (1)$$

Figure 4(c) shows that Eq. (1) with $A=0.47$, $t_i=20$ fs, and $\tau=413$ fs fits the TDDFT results reasonably well. The inset in Fig. 4(c) shows that within 2 ps, about 0.77 electrons are transferred to Tl. We can qualitatively understand the amount of electron transfer as follows: In the Ehrenfest dynamics, the excited electron state evolves into a superposed state between $|\mathrm{CBM}\rangle$ and $|\mathrm{Tl},p_i\rangle$,

$$|\varphi\rangle = a|\mathrm{CBM}\rangle + b_1|\mathrm{Tl},p_1\rangle + b_2|\mathrm{Tl},p_2\rangle + b_3|\mathrm{Tl},p_3\rangle \quad (2)$$

with approximately the same energy. If we assume $|a|^2 = |b_1|^2 = |b_2|^2 = |b_3|^2 = 1/4$, we get $\Delta\rho_{\mathrm{Tl}} = 3/4 = 0.75$ electrons. Note that this discussion considers only a single Tl. If we take into account the coupling of the delocalized $|\mathrm{CB}\rangle$ with multiple (n) Tl atoms nearby, the amount of the electron transfer in the first 2 ps will increase to $\Delta\rho_{\mathrm{Tl}} = 1-1/(3n+1)$, which approaches 1 in the limit $n\to\infty$. This suggests that the excited electron transfer from CBM to Tl is considerably faster than the NRR in CsI by at least several orders of magnitude.

To calculate the NRR barrier for Tl-doped CsI, we use PBE0 but with an excited electron in the Tl p state as shown in Fig. 3(b). The energy difference between STE and $(V_{\mathrm{I}}\text{-}\mathrm{I}_i^{\mathrm{DB}})^{\mathrm{second}}$ increases to ~0.54 eV, which is 0.25 eV higher than that for undoped CsI. One can estimate the reduction in the NRR rate by $R=\exp(\Delta E_b/kT)$. Using $\Delta E_b = 0.63-0.30 = 0.33$ eV and $kT=0.026$ eV, we obtain $R=3\times10^5$ at RT. The corresponding NRR time is roughly 1 ms, which is enough to significantly increase light output.

V. IMPLICATION TO SEMICONDUCTORS

Note that the mechanism to deter NRR (discussed above) is not limited to only alkali halides or to ionic insulators. For example, carrier trapping by BO_2 complexes in Si has been proposed as the main reason for NRR in B-doped Czochralski Si (Cz-Si) solar cell materials.[37] What is intriguing for this system is the lack of deep levels similar to CsI; electrons and holes that are temporarily trapped at near band-edge BO_2 states assist the NRR.[38] It is thus conceivable that one may reduce carrier trapping in Cz-Si by introducing impurities that are capable of taking the carriers away from BO_2.

VI. SUMMARY

Hybrid functional study, coupled with TDDFT, reveals the effect of impurity doping on excited carrier relaxation in ionic insulators. Application to Tl-doped CsI explains the experimentally observed significant increase of scintillation efficiency. The role of the impurity in suppressing NRR is unveiled in terms of the efficient transfer of excited electrons to impurity gap states. Our results suggest that defects/impurities not only can accelerate NRR as often observed,[4,5,38] but can also be used to suppress certain NRRs, provided that the NRR does not involve deep levels as in the Shockley-Read-Hall regime.[4,5] In other words, our understanding of the physics to deter NRR goes beyond just the improvement of current scintillator technology, but for educated defect engineering to suppress NRR in other optoelectronic materials.

ACKNOWLEDGMENTS

This work was supported by the National Nuclear Security Administration, Office of Nuclear Nonproliferation Research and Engineering (NA-22), of the US Department of Energy and by the Computational Center for Nanotechnology Innovations at RPI. F.G. and Z.G.W. acknowledge the use of the supercomputers in the Environmental Molecular Sciences Laboratory, a national scientific user facility sponsored by the US Department of Energy's Office of Biological and Environmental Research. S.M. is grateful for support from NSFC (Grants No. 11074287 and No. 11222431) and MOST (2012CB921403).

[1] A. M. Stoneham, Rep. Prog. Phys. **44**, 1251 (1981).
[2] C. Deibel, T. Strobel, and V. Dyakonov, Adv. Mater. **22**, 4097 (2010).
[3] D. Hertel, S. Setayesh, H.-G. Nothofer, U. Scherf, K. Müllen, and H. Bässler, Adv. Mater. **13**, 65 (2001).
[4] W. Shockley and W. T. Read, Phys. Rev. **87**, 835 (1952).
[5] R. N. Hall, Phys. Rev. **87**, 387 (1952).
[6] M. Nikl, Phys. Status Solidi A **178**, 595 (2000).
[7] N. Yasui, Y. Ohashi, T. Kobayashi, and T. Den, Adv. Mater. **24**, 5464 (2012).
[8] P. Schotanus, R. Kamermans, and P. Dorenbos, IEEE Trans. Nucl. Sci. **37**, 177 (1990).
[9] M. M. Hamada, F. E. Costa, M. C. C. Pereira, and S. Kubota, IEEE Trans. Nucl. Sci. **48**, 1148 (2001).
[10] Z. Wang, Y. Xie, B. D. Cannon, L. W. Campbell, F. Gao, and S. Kerisit, J. Appl. Phys. **110**, 064903 (2011).
[11] S. Kerisit, K. M. Rosso, and B. D. Cannon, IEEE Trans. Nucl. Sci. **55**, 1251 (2008).
[12] S. Kerisit, K. M. Rosso, B. D. Cannon, F. Gao, and Y. Xie, J. Appl. Phys. **105**, 114915 (2009).
[13] S. Zazubovich, Radiat. Meas. **33**, 699 (2001).
[14] J. M. Spaeth, W. Meise, and K. S. Song, J. Phys.: Condens. Matter **6**, 3999 (1994).
[15] V. Nagirnyi, A. Stolovich, S. Zazubovich, V. Zepelin, E. Mihokova, M. Nikl, G. P. Pazzi, and L. Salvini, J. Phys.: Condens. Matter **7**, 3637 (1995).
[16] V. Babin, P. Fabeni, K. Kalder, M. Nikl, G. P. Pazzi, and S. Zazubovich, Radiat. Meas. **29**, 333 (1998).
[17] J. P. Perdew, M. Emzerhof, and K. Burke, J. Chem. Phys. **105**, 9982 (1996).
[18] G. Kresse and J. Furthmuller, Comput. Mater. Sci. **6**, 15 (1996).
[19] P. E. Blochl, Phys. Rev. B **50**, 17953 (1994).

[20]E. Runge and E. K. U. Gross, Phys. Rev. Lett. **52**, 997 (1984).
[21]J. M. Soler, E. Artacho, J. D. Gale, A. García, J. Junquera, P. Ordejón, and D. Sánchez-Portal, J. Phys.: Condens. Matter **14**, 2745 (2002).
[22]S. Meng and E. Kaxiras, J. Chem. Phys. **129**, 054110 (2008).
[23]N. Troullier and J. L. Martins, Phys. Rev. B **43**, 1993 (1991).
[24]J. P. Perdew, K. Burke, and M. Ernzerhof, Phys. Rev. Lett. **77**, 3865 (1996).
[25]R. M. V. Ginhoven, J. E. Jaffe, S. Kerisit, and K. M. Rosso, IEEE Trans. Nucl. Sci. **57**, 2303 (2010).
[26]S. E. Derenzo and M. J. Weber, Nucl. Instrum. Methods Phys. Res., Sect. A **422**, 111 (1999).
[27]G. Blasse, Chem. Mater. **6**, 1465 (1994).
[28]M. Nikl, Meas. Sci. Technol. **17**, R37 (2006).
[29]G. Bizarri, J. Cryst. Growth **312**, 1213 (2010).
[30]A. I. Popov, E. A. Kotomin, and J. Maier, Nucl. Instrum. Methods Phys. Res., Sect. B **268**, 3084 (2010).
[31]N. Itoh, Adv. Phys. **31**, 491 (1982).
[32]N. Itoh, A. M. Stoneham, and A. H. Harker, J. Phys. C **10**, 4197 (1977).
[33]J. F. Vetelino, K. V. Namjoshi, and S. S. Mitra, Phys. Rev. B **7**, 4001 (1973).
[34]C. Amsler, D. Grögler, W. Joffrain, D. Lindelöf, M. Marchesotti, P. Niederberger, H. Pruys, C. Regenfus, P. Riedler, and A. Rotondi, Nucl. Instrum. Methods Phys. Res., Sect. A **480**, 494 (2002).
[35]TDDFT results in Fig. 4(a) reflect the splitting and lowering of the Tl p states due to symmetry breaking by the MD.
[36]W. R. Duncan and O. V. Prezhdo, Annu. Rev. Phys. Chem. **58**, 143 (2007).
[37]J. Schmidt and K. Bothe, Phys. Rev. B **69**, 024107 (2004).
[38]M.-H. Du, H. M. Branz, R. S. Crandall, and S. B. Zhang, Phys. Rev. Lett. **97**, 256602 (2006).